The EMBO Journal (2009) 28, 2896–2907 | © 2009 European Molecular Biology Organization | All Rights Reserved 0261-4189/09
www.embojournal.org

THE EMBO JOURNAL

A non-redundant role for MKP5 in limiting ROS production and preventing LPS-induced vascular injury

Feng Qian[1], Jing Deng[1], Ni Cheng[1], Emily J Welch[1], Yongliang Zhang[2], Asrar B Malik[1], Richard A Flavell[3], Chen Dong[2] and Richard D Ye[1,]*

[1]Department of Pharmacology, University of Illinois College of Medicine, Chicago, IL, USA, [2]Department of Immunology, University of Texas MD Anderson Cancer Center, Houston, TX, USA and [3]Department of Immunobiology and Howard Hughes Medical Institute, Yale University School of Medicine, New Heaven, CT, USA

There are at least 11 mitogen-activated protein kinase (MAPK) phosphatases (MKPs) and only 3 major groups of MAPKs, raising the question of whether these phosphatases have non-redundant functions *in vivo*. Using a modified mouse model of local Shwartzman reaction, we found that deletion of the MKP5 gene, but not the MKP1 gene, led to robust and accelerated vascular inflammatory responses to a single dose of LPS injection. Depletion of neutrophils significantly reduced the vascular injury in *Mkp5*$^{-/-}$ mice, whereas adoptive transfer of *Mkp5*$^{-/-}$ neutrophils replicated the LPS-induced skin lesions in wild-type recipients. Neutrophils isolated from *Mkp5*$^{-/-}$ mice exhibited augmented p38 MAPK activation and increased superoxide generation on activation. The p38 MAPK inhibitor, SB203580, significantly reduced p47^{phox} phosphorylation and diminished superoxide production in neutrophils. p38 MAPK phosphorylated mouse p47^{phox}, and deletion of the p47^{phox} gene ablated the LPS-induced vascular injury in *Mkp5*$^{-/-}$ mice. Collectively, these results show an earlier unrecognized and non-redundant function of MKP5 in restraining p38 MAPK-mediated neutrophil oxidant production, thereby preventing LPS-induced vascular injury.

The EMBO Journal (2009) **28,** 2896–2907. doi:10.1038/emboj.2009.234; Published online 20 August 2009
Subject Categories: signal transduction; immunology
Keywords: LPS; MAPK; MKP5; NADPH oxidase; neutrophils

Introduction

Mitogen-activated protein kinases (MAPKs), including extracellular signal-regulated protein kinases (ERK), p38 MAPK and c-Jun N-terminal kinases (JNK), are activated through dual phosphorylation of their tripeptide motifs Thr-Glu-Tyr (ERK), Thr-Gly-Tyr (p38) and Thr-Pro-Tyr (JNK) within the activation loop (reviewed in Chen *et al*, 2001; Morrison and Davis, 2003). Dual phosphorylation of the Thr and Tyr residues is mediated through a highly conserved protein kinase cascade. In mammalian cells, ERK is activated by the MAPK kinases MKK1 and MKK2, p38 MAPK is activated by MKK3, MKK4 and MKK6 and JNK is activated by MKK4 and MKK7. There are also upstream kinases that respond to growth factors, inflammatory cytokines and stress signals and activate these MAPK kinases (Dong *et al*, 2002). The activated MAPKs then translocate to the nucleus and serve important functions in transcriptional regulation. In immune cells such as T lymphocytes and macrophages, MAPKs can be activated by inflammatory cytokines including TNF-α and IL-1β. These cells also respond to bacterial products including LPS and formylated chemotactic peptides with potent activation of selected MAPKs. As a result of these signalling events, MAPKs regulate the development, differentiation and activation of T lymphocytes as well as cytokine production in macrophages. The physiological importance and complexity of the MAPK cascade is evidenced by the presence of multiple forms of the MAPKs within each group, and by the profound effects that MAPK inhibition or gene deletion produce *in vitro* and *in vivo* (Chen *et al*, 2001).

Given the important functions of MAPKs in all mammalian cells, proper regulation of their activities is crucial. Protein kinase phosphatases that act on either the phosphorylated threonines (e.g. PP2A, PP2C) or the phosphoylated tyrosines (e.g. PTPN5, PTPN7 and PTPRR) in activated MAPKs are the functional phosphatases for MAPKs (Alessi *et al*, 1995; Keyse, 2000; Farooq and Zhou, 2004). Dual specificity phosphatases (DUSPs) are MAP kinase phosphatases (MKPs) that selectively dephosphorylate both the phosphorylated threonines and phosphorylated tyrosines in activated MAPKs, a reaction involving the active site Cys and Asp residues in a MKP (Sun *et al*, 1993; Camps *et al*, 2000; Bhalla *et al*, 2002; Farooq and Zhou, 2004; Lang *et al*, 2006; Jeffrey *et al*, 2007; Liu *et al*, 2007; Zhang and Dong, 2007). Since the discovery of MKP1 (Sun *et al*, 1993), a total of 11 DUSPs have been identified as MKPs (Lang *et al*, 2006; Jeffrey *et al*, 2007; Liu *et al*, 2007; Zhang and Dong, 2007). These MKPs are expressed broadly in tissues and localized to different subcellular compartments (Camps *et al*, 2000; Farooq and Zhou, 2004). The fact that the number of available MKPs exceeds the number of MAPKs suggests different regulatory mechanisms for MKPs, which may lie in their substrate specificity, induced expression and tissue distribution. *In vitro* studies have shown that MKP1 and MKP5 share similar substrate specificities (p38 MAPK $\approx$ JNK $>$ ERK), although MKP5 has an extra fragment N-terminal to its catalytic domain and belongs to a different subfamily of DUSPs (Tanoue *et al*, 1999; Theodosiou *et al*, 1999; Farooq and Zhou, 2004). There are also reports suggesting that the *in vitro* substrate selectivity of an MKP may differ from its selectivity *in vivo* (Lang *et al*, 2006; Jeffrey

*Corresponding author. Department of Pharmacology, University of Illinois at Chicago, 835 South Wolcott Avenue, M/C 868, Chicago, IL 60612, USA. Tel.: +1 312 996 5087; Fax: +1 312 996 7857; E-mail: yer@uic.edu

Received: 1 April 2009; accepted: 22 July 2009; published online: 20 August 2009

et al, 2007; Liu *et al*, 2007; Zhang and Dong, 2007). Therefore, it is presently unclear whether these MKPs have unique spatial and temporal characteristics or are functionally redundant.

Recent studies using genetically altered mice lacking MKP1 (Zhao *et al*, 2005, 2006; Salojin *et al*, 2006), MKP5 (Zhang *et al*, 2004) and PAC1 (Jeffrey *et al*, 2006) have shown that these MKPs have important functions in regulating the expression of pro-inflammatory and immunomodulatory cytokines. These regulatory functions of MKPs are mediated through their suppression of the transcription-stimulating activities of the MAPKs. However, it was unclear whether MKPs regulate the activities of MAPKs in cytosolic compartment. In this study, we used a modified mouse model of local Shwartzman reaction (LSR) to examine a role of MKP5 in regulating host responses to inflammatory stimuli. LSR is a delayed vascular response to bacterial LPS and the inflammatory cytokine TNF-α, and is induced by consecutive injections of LPS (or LPS followed by TNF-α) into the skin of rabbits and mice (Stetson and Good, 1951; Brozna, 1990). As MAPKs are critical downstream effectors of the LPS signalling cascade, the LSR is an appropriate model for investigating the potential functions of MKPs in regulating inflammatory cell activation. Our results show a non-redundant function of MKP5 in the protection against LPS-induced vascular injury resulting from excessive p38 MAPK activation and neutrophil superoxide production.

Results

LPS induces a robust and accelerated vascular response in mice lacking MKP5

We used a mouse model of LSR to examine the physiological roles of MKP5 in maintaining homeostasis of host response to bacterial toxins and protection against tissues injury. In the classic LSR (Stetson and Good, 1951; Brozna, 1990), two injections of LPS separated by 18–24 h, or an LPS injection followed by a TNF-α injection 18–24 h later (Figure 1A), were required to induce skin lesions resembling those of thrombohaemorrhagic vasculitis. Surprisingly, all *Mkp5*$^{-/-}$ mice examined (15/15) reacted strongly to the first injection of LPS, which did not induce macroscopic lesions in WT mice (Figure 1A). Haemorrhage and dermal tissue necrosis was visible at the injection site 24 h after a single LPS administration (Figure 1B, left panels), and the extent of haemorrhage was quantified (Figure 1C). In contrast, mice lacking MKP1, which exhibits substrate specificity similar to that of MKP5, did not display exaggerated vascular response to LPS (Figure 1B, right panels). The *Mkp1*$^{-/-}$ mice responded similarly to their WT littermates in the classic LSR after the second injection (data not shown). Histological examination of dermal tissues from the *Mkp5*$^{-/-}$ mice showed erythrocyte extravasation, microcapillary thrombus formation and neutrophil accumulation at the site of LPS injection (Figure 1D, lower right image). No vascular injury and skin lesions were observed at the site of PBS injection in the same animals.

Mkp5$^{-/-}$ *neutrophils are necessary for the augmented vascular response to LPS*

Neutrophil infiltration at the LPS injection site was quantified based on neutrophil myeloperoxidase (MPO) activity. As shown in Figure 2A, increased MPO activity was detectable in *Mkp5*$^{-/-}$ mice 12 and 24 h after LPS injection. However, peripheral blood neutrophil counts in WT and *Mkp5*$^{-/-}$ (KO) mice were similar (Figure 2B), suggesting increased neutrophil infiltration but not expansion of the neutrophil pool in the *Mkp5*$^{-/-}$ mice. Using an air pouch model, we determined pro-inflammatory chemokine and cytokine expression. LPS induced significantly more secretion of TNF-α, keratinocyte-derived chemokine (KC) and IL-6 in the *Mkp5*$^{-/-}$ mice than in WT littermates (Figure 2C–E). Elevated KC level could contribute to neutrophil accumulation at the LPS injection site.

To determine whether neutrophil accumulation is critical to the LPS-induced vascular inflammation, anti-Gr-1 antibody was administered intraperitoneal (i.p.) to deplete neutrophils. The antibody effectively reduced neutrophil count in peripheral blood by $\sim$85%, whereas an isotype-matched IgG control produced no significant change in 48 h ($P<0.01$; Figure 3A). *Mkp5*$^{-/-}$ mice that received anti-Gr-1 or an IgG control were then given either LPS or PBS. As shown in Figure 3B, mice receiving anti-Gr-1 displayed significantly reduced ($P<0.05$) loss of MPO activity at the site of LPS injection, suggesting reduced neutrophil infiltration. Mice receiving anti-Gr-1 also showed diminished skin lesions on LPS stimulation, with reduced haemorrhage (Figure 3C). These results indicate that local accumulation of neutrophils is necessary for the LPS-induced vascular inflammatory response in the *Mkp5*$^{-/-}$ mice.

Administration of the anti-Gr-1 antibody resulted in a small decrease in peripheral monocytes count, as the antibody used recognizes a subset of monocytes. The change in monocytes count, however, is not statistically significant (Supplementary Figure S1A). To determine whether neutrophils are the primarily contributor to the LPS-induced tissue damage in *Mkp5*$^{-/-}$ mice, we adoptively transferred *Mkp5*$^{-/-}$ neutrophils to recipient WT mice. Transfer of *Mkp5*$^{-/-}$ bone marrow-derived neutrophils, but not WT neutrophils, reconstitutes the thrombohaemorrhagic lesions in WT recipients on LPS stimulation. Moreover, the extent of LPS-induced haemorrphage was positively correlated with the number of neutrophils transferred (Figure 3D and E). As the bone marrow-derived neutrophils were approximately 78% Gr-1^{+}, we further determined whether neutrophils or other cell populations were responsible for the observed skin lesions, using flow cytometry to enrich the neutrophil population to $>$99% purity (Supplementary Figure S1B and C). When adoptively transferred to the recipient mice, these neutrophils produced results similar to those in Figure 3D and E (Supplementary Figure S2). On the basis of these findings, we conclude that the *Mkp5*$^{-/-}$ neutrophils are both necessary and sufficient for the LPS-induced vascular injury in mice.

Loss of Mkp5 leads to augmented neutrophil superoxide production

The ability to release granule contents and produce superoxide by activated neutrophils is essential to host defence against invading microbial pathogens. These bactericidal functions, however, also contribute to vascular injury in many inflammatory diseases. In a classic LSR, vascular injury resulting from LPS and TNF-α injections depends on the release of neutrophil elastase and requires activation of a complement C3-triggered, Mac-1-dependent signalling pathway (Hirahashi *et al*, 2006). Although neutrophil-derived superoxide and other oxygen radicals are highly toxic to

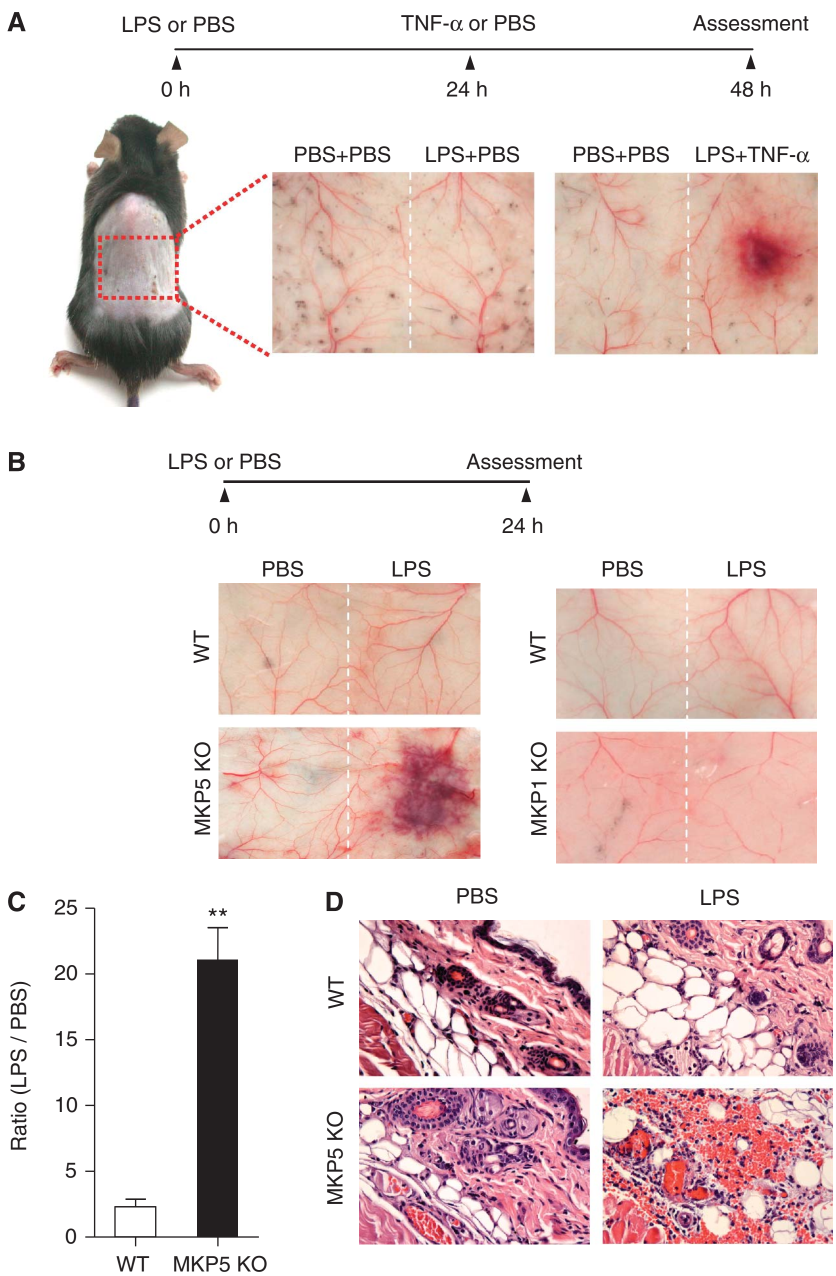

Figure 1 LPS-induced microvascular injury in $Mkp5^{+/+}$ and $Mkp5^{-/-}$ mice. (**A**) Experimental scheme and results of a classical local Shwartzman reaction (LSR) induced by consecutive injections of LPS and then TNF-α. Dorsal skin of WT mice were first injected s.c. with LPS (80 μg, right side of each panel) or PBS control (left side). After 24 h, TNF-α (0.2 μg) or PBS in same volume was injected s.c. into the same site that received LPS. The mice were killed 24 h after the second injection, and the skin tissues were examined macroscopically. Representative sample images from one of the five experiments are shown. (**B**) Experimental scheme and results of a modified (one-injection) LSR showing macroscopic appearance of dorsal skin in $Mkp5^{+/+}$ (WT) and $Mkp5^{-/-}$ (KO) mice (panels on the left), compared with that of the $Mkp1^{+/+}$ (WT) and $Mkp1^{-/-}$ (KO) mice (panels on the right). The WT and KO littermates in each group received an injection of either LPS (80 μg; right to the dotted line) or PBS (left to the dotted line). A total of 11 WT and 15 $Mkp5^{-/-}$ mice, and 8 WT and 8 $Mkp1^{-/-}$ mice were examined 24 h after the LPS injection. Representative images are shown. (**C**) The degree of haemorrhage in the $Mkp5^{+/+}$ and $Mkp5^{-/-}$ group above was estimated based on densitometry analysis of skin samples receiving either LPS or PBS injection. $^{**}P<0.01$. (**D**) Grouped images showing representative photomicrographs of H&E-stained skin sections from WT (upper panels) and $Mkp5^{-/-}$ (lower panels) mice that were treated with LPS or PBS as marked. Erythrocyte extravasation, thrombus formation and neutrophil accumulation are evident in the sample from LPS-treated $Mkp5^{-/-}$ mice 24 h after LPS injection.

bacteria as well as mammalian cells (Nauseef, 2007), a role for oxygen radicals in LSR has not been established. To determine whether major bactericidal activities were altered in $Mkp5^{-/-}$ neutrophils, we conducted chemotaxis assay using the mouse chemokine KC. Both WT and $Mkp5^{-/-}$ neutrophils behaved similarly in chemotaxis towards KC (Supplementary Figure S3A). These neutrophils also responded to C5a, an anaphylatoxin with a demonstrated role in the LSR and septic responses (Shin *et al*, 1968; Rothstein *et al*, 1988), in chemotaxis and degranulation assays, with no significant difference between the WT and $Mkp5^{-/-}$ mice (Supplementary Figure S3B and C). Likewise, fMet-Leu-Phe

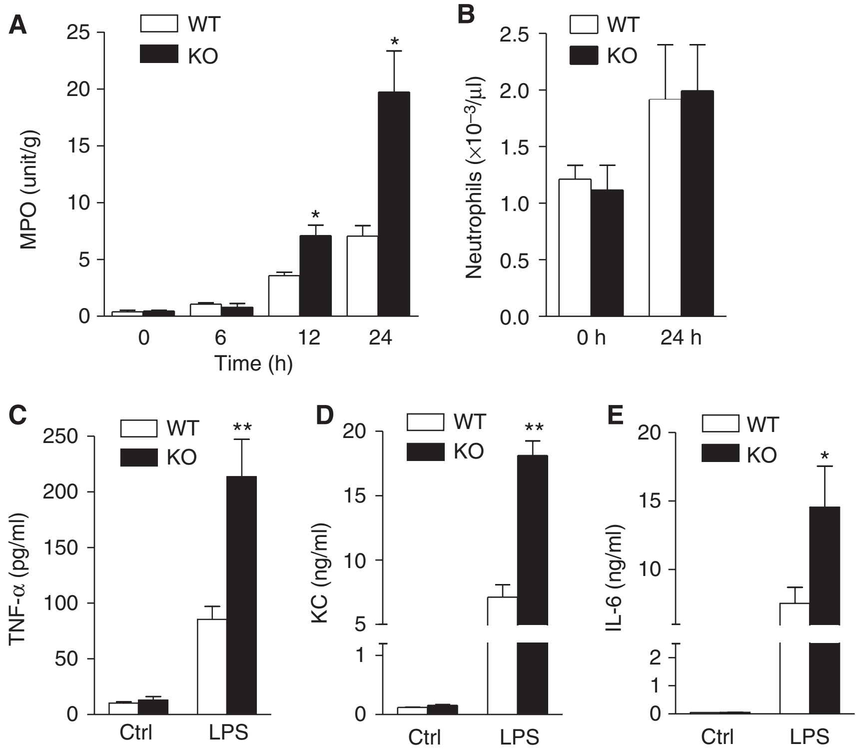

Figure 2 LPS-induced tissue neutrophilia and cytokine production in *Mkp5*$^{+/+}$ and *Mkp5*$^{-/-}$ mice. (**A**) Time-dependent neutrophil accumulation at the LPS injection sites in WT and *Mkp5*$^{-/-}$ (KO) mice, based on the activity of neutrophil myeloperoxidase (MPO) in tissue extract. The values of MPO activity represent the means ± s.e.m. of measurements in four mice. The difference between the WT and KO mice at 12 and 24 h time points was statistically significant (*$P<0.05$). (**B**) Peripheral blood neutrophil count in WT and *Mkp5*$^{-/-}$ (KO) mice before (0 h) and after (24 h) receiving 80 μg LPS ($n=5$). (**C–E**) Change in the expression level of TNF-α, KC and IL-6 in WT and *Mkp5*$^{-/-}$ mice. Air pouch was established by injecting sterile air into the dorsal skin of WT and *Mkp5*$^{-/-}$ (KO) mice. LPS (80 μg) was then injected into the air pouch. After 2 h, lavage fluid was collected from the air pouch and the concentration of TNF-α, KC and IL-6 was determined. Values shown are means ± s.e.m. of measurements using four mice. *$P<0.05$ and **$P<0.01$, compared with LPS-stimulated WT mice.

(fMLF) induced similar chemotaxis and β-glucuronidase release in *Mkp5*$^{-/-}$ mice and WT littermates (Supplementary Figure S4A and B). In contrast, neutrophils from the *Mkp5*$^{-/-}$ mice produced significantly more superoxide than neutrophils from the WT littermates when stimulated with C5a (Figure 4A). Interestingly, neutrophils from the *Mkp1*$^{-/-}$ mice showed no difference from their WT littermates in C5a-induced superoxide production (Figure 4B). The *Mkp5*$^{-/-}$ neutrophils also exhibited enhanced superoxide production in response to TNF-α stimulation (Figure 4C), and adherence to fibrinogen-coated surface further increased and extended the superoxide production (Figure 4D). These changes were also observed in *Mkp5*$^{-/-}$ neutrophils stimulated with fMLF and the phorbol ester PMA (Supplementary Figure S4C and D), suggesting that MKP5 deficiency broadly altered neutrophil superoxide production induced by soluble activators of NADPH oxidase. Together, these results indicate that MKP5, but not MKP1, has a function in the negative regulation of neutrophil NADPH oxidase.

Augmented superoxide production and vascular injury in Mkp5$^{-/-}$ *neutrophils require activation of p38 MAPK*

To delineate the mechanisms by which MKP5 protects vascular cells from LPS-induced damage, we sought to determine the effect of *Mkp5* deletion on MAPK activation in neutrophils. Studies conducted *in vitro* suggest that MKP5 preferentially dephosphorylates activated MAPKs in the order of p38 MAPK≈JNK>ERK (Tanoue *et al*, 1999; Theodosiou *et al*, 1999). To determine the effect of *Mkp5* deletion in MAPK activation in intact cells, neutrophils were purified from the *Mkp5*$^{-/-}$ and WT mice and stimulated with C5a (10 nM). Phosphorylation of MAPK was determined by western blotting using specific anti-phospho-MAPK antibodies. Under these experimental conditions, the *Mkp5*$^{-/-}$ neutrophils exhibited enhanced ERK phosphorylation with unaltered kinetics that promptly terminate after 2 min (Figure 5A). No significant changes in JNK phosphorylation beyond a slightly increased basal level were observed in *Mkp5*$^{-/-}$ neutrophils (Figure 5B). In contrast, C5a stimulated a sustained increase in p38 MAPK phosphorylation in the *Mkp5*$^{-/-}$ neutrophils compared with neutrophils from WT littermate (Figure 5C). The changes in the MAPK phosphorylation pattern suggest that MKP5 selectively regulates p38 MAPK activation and produces lesser effects on ERK and JNK activation in neutrophils.

We postulated that C5a produced at the site of LPS injection could stimulate enhanced superoxide generation in the *Mkp5*$^{-/-}$ neutrophils through hyperactivation of p38 MAPK. This possibility was examined *ex vivo* using pharmacological inhibitors for MAPKs. As shown in Figure 5D, the enhanced superoxide production in *Mkp5*$^{-/-}$ neutrophils was ablated with the p38 MAPK inhibitor SB203580 ($P<0.01$). In contrast, SP600125 and PD98059, inhibitors for the JNK and ERK signalling pathways, respectively, produced no significant

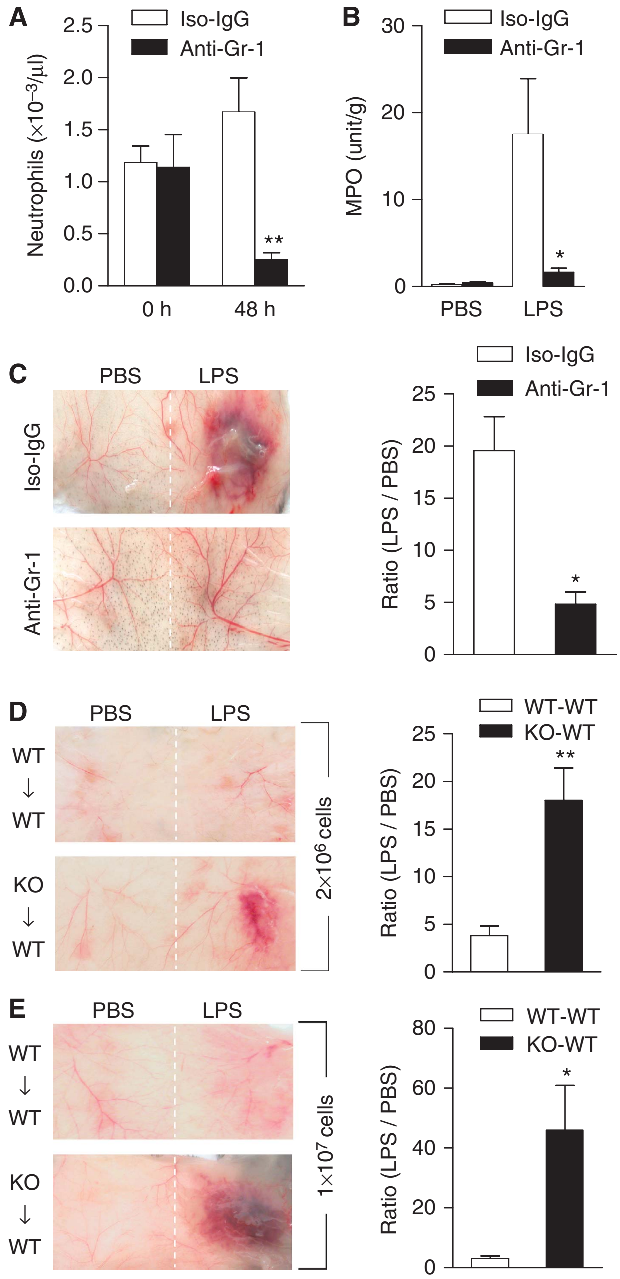

Figure 3 Role of neutrophils in LPS-induced microvascular injury in *Mkp5*$^{-/-}$ mice. (**A**) Peripheral blood neutrophil count showing anti-Gr-1-mediated depletion of neutrophils in *Mkp5*$^{-/-}$ mice, determined at 0 and 48 h after i.p. injection of the antibody (filled bars) and compared with mice receiving isotype-matched IgG (Iso-IgG, open bars). (**B**) Neutrophil accumulation at the site of LPS or PBS injection in *Mkp5*$^{-/-}$ mice receiving anti-Gr-1 (filled bars) or isotype-matched IgG (open bars). (**C**) Macroscopic appearance of dorsal skin in LPS-injected *Mkp5*$^{-/-}$ mice that received anti-Gr-1 or isotype-matched IgG (100 μg each) 24 h before LPS challenge. Representative images from five independent experiments are shown. The degree of haemorrhage was quantified by densitometry and shown on the right side. (**D**, **E**) WT mice were intravenously injected with bone marrow neutrophils (2×10^6 in D, and 1×10^7 in E) isolated from either *Mkp5*$^{-/-}$ mice (KO to WT) or WT mice (WT to WT). After 10 min, dorsal skin was injected s.c. with LPS (80 μg). Macroscopic appearance of the LPS injection site was imaged at 24 h ($n=5$ in each group), and representative images are shown. For (C), (D) and (E), the degree of haemorrhage was estimated by densitometry as described in Figure 1, and the results are shown as means ± s.e.m. on the right side of the images. $^*P<0.05$; $^{**}P<0.01$, based on five mice in each group.

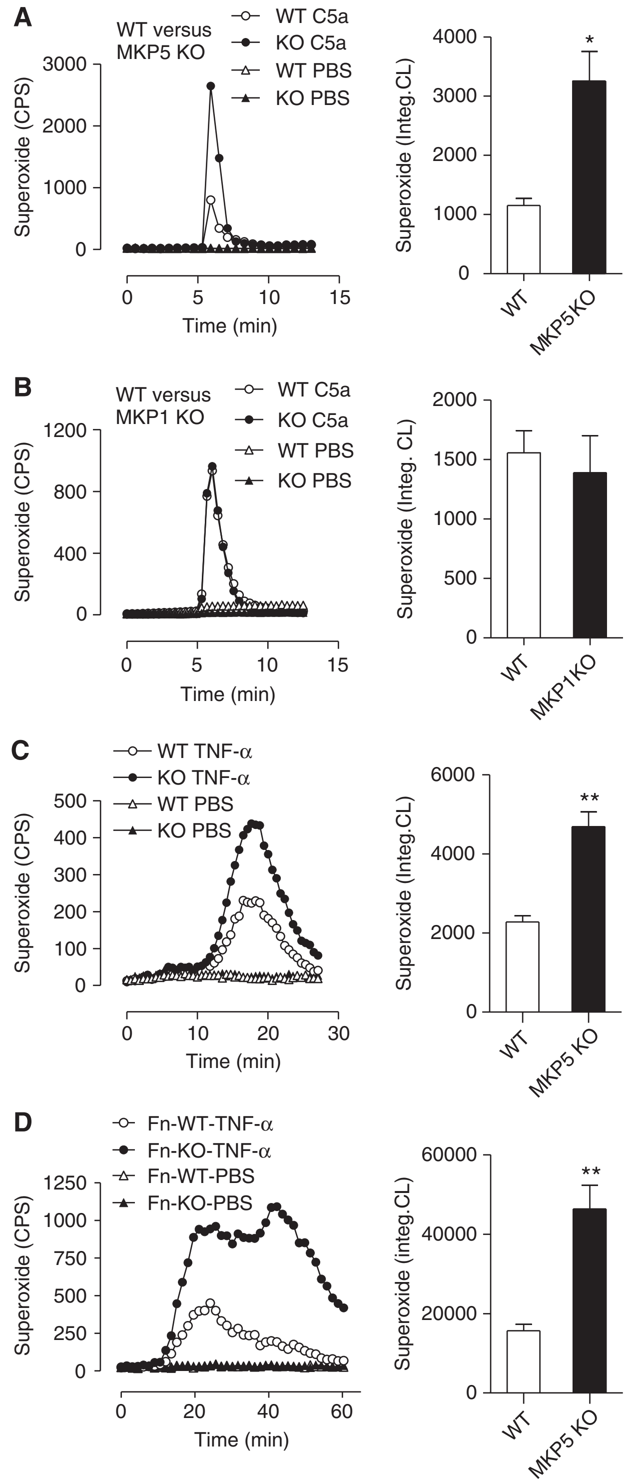

Figure 4 Augmented superoxide production in *Mkp5*$^{-/-}$ neutrophils. Representative tracings showing the production of superoxide as counts per second (CPS) by neutrophils (5×10^5) from the *Mkp5*$^{-/-}$ mice (**A**), *Mkp1*$^{-/-}$ mice (**B**) and their WT littermates, stimulated in suspension with 100 nM C5a or PBS. In (**C**) neutrophils from the *Mkp5*$^{-/-}$ mice and their WT littermates were stimulated with 100 ng/ml TNF-α or PBS, and superoxide production was measured. In (**D**) neutrophils from *Mkp5*$^{-/-}$ mice and their WT littermates were let adherent to fibrinogen-coated surface and stimulated with 100 ng/ml TNF-α. Superoxide generation in these experiments was detected using isoluminol-ECL. Shown on the right to the tracings are quantifications of cumulative superoxide production as means ± s.e.m., based on measurement of integrated chemiluminescence (CL) in the course of the assays as indicated ($n=5$). $^*P<0.05$; $^{**}P<0.01$.

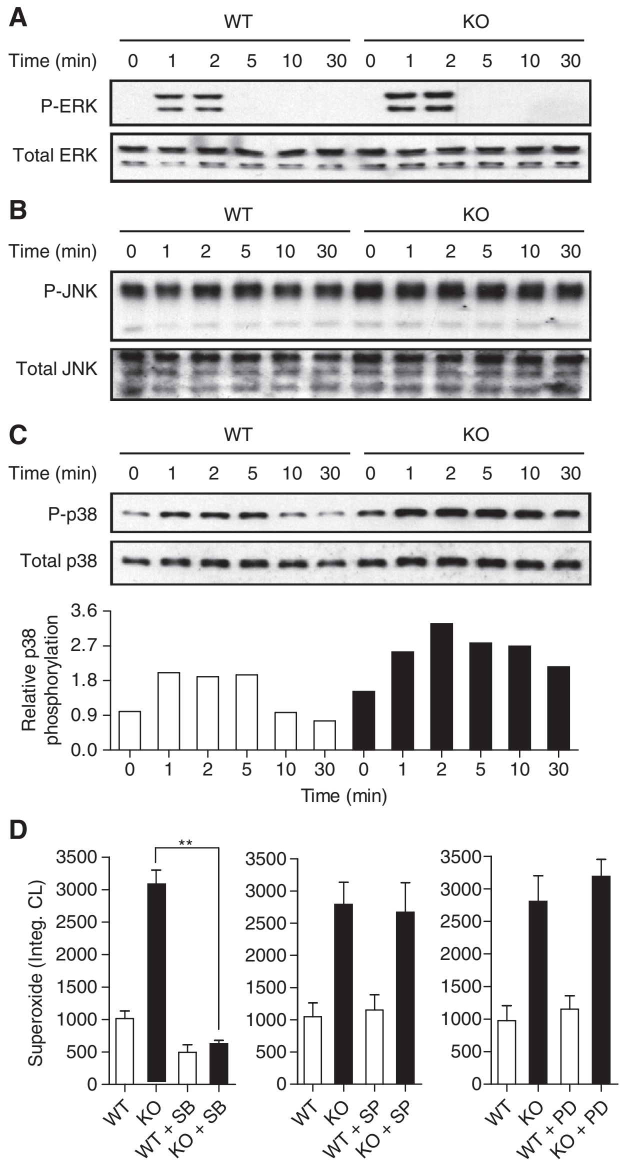

Figure 5 C5a-induced MAPK activation and superoxide production in WT and *Mkp5*$^{-/-}$ neutrophils. Phosphorylation of ERK1/2 (**A**), JNK (**B**) and p38 MAPK (**C**) in C5a (10 nM)-stimulated WT and *Mkp5*$^{-/-}$ neutrophils was determined by western blotting using anti-phospho-antibodies against the individual MAPKs. Total MAPKs in the samples were shown below the phospho-MAPK blots. Densitometry analysis was conducted to determine the relative level of induced p38 MAPK phosphorylation, and the results are shown in (C). (**D**) The effects of MAPK inhibitors on C5a-stimulated superoxide production in WT (open bars) and *Mkp5*$^{-/-}$ (KO, filled bars) neutrophils, shown as integrated chemiluminescence (CL) in a 15 min period after stimulation. The cells were treated for 15 min with either the p38 MAPK inhibitor SB203580 (SB, 3 μM), the JNK inhibitor SP600125 (SP, 10 μM) or the MEK inhibitor PD98059 (PD, 30 μM), before C5a stimulation. Data shown are means ± s.e.m. from three independent experiments. $^{**}P<0.01$.

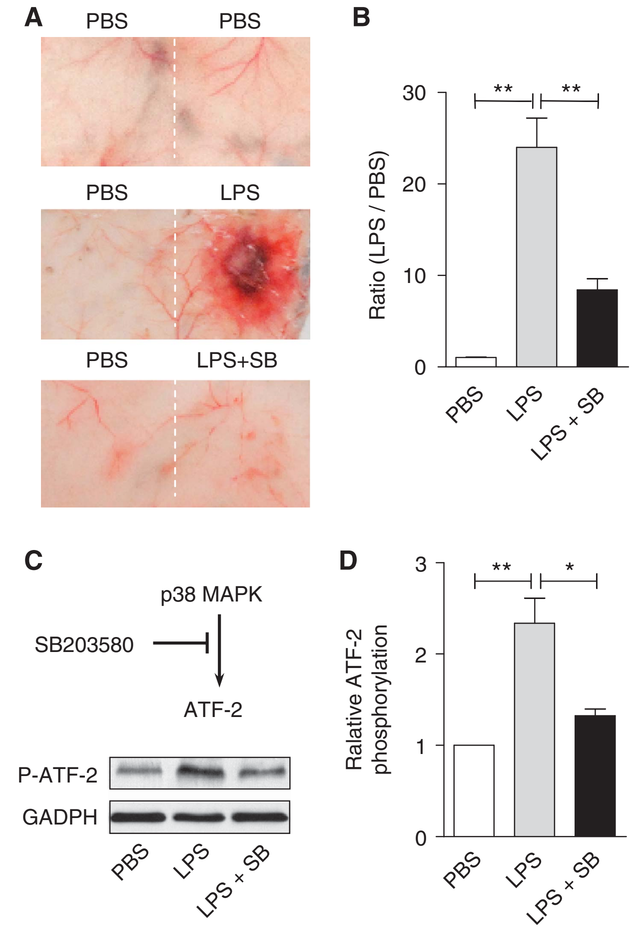

Figure 6 *In vivo* effects of SB203580 on LPS-induced vascular injury and p38 MAPK activation. The p38 MAPK inhibitor SB203580 (100 μg) was co-administered s.c. with LPS (80 μg) to *Mkp5*$^{-/-}$ mice. Control mice received either PBS or LPS alone. The mice were killed 24 h after injection, and skin tissue at the injection site was examined (**A**). The degree of a haemorrhage was quantified by densitometry analysis of skin sample and shown in (**B**). (**C**) Skin tissues at the injection site were excised and ATF-2 phosphorylation in tissue homogenate was determined by western blotting, using an antibody recognizing phosphorylated ATF-2. The relative level of ATF-2 phosphorylation was shown in (**D**). $^{**}P<0.01$ and $^{*}P<0.05$, based on four experiments.

effect on C5a-induced superoxide generation in either WT or *Mkp5*$^{-/-}$ neutrophils (Figure 5D, middle and right panels). Taken together, these results show that p38 MAPK, but not JNK and ERK, is a primary target of MKP5 in regulating neutrophil superoxide production.

We next determined whether inhibition of p38 MAPK could affect the LPS-induced skin lesions *in vivo*. *Mkp5*$^{-/-}$ mice were given LPS alone or LPS and SB203580 together. As shown in Figure 6A and B, co-administration of SB203580 and LPS to *Mkp5*$^{-/-}$ mice significantly reduced skin lesions compared with mice receiving LPS alone ($P<0.01$). Injection of SB203580 together with LPS markedly decreased the LPS-induced ATF-2 phosphorylation (Figure 6C and D), showing that pharmacological inhibition of p38 MAPK could effectively block the exacerbated LSR.

Mkp5 deletion increases p38 MAPK-mediated phosphorylation of mouse p47^{phox}

Phosphorylation of p47^{phox} leads to conformational changes necessary for its membrane translocation. Biochemical characterization of human p47^{phox} has led to the identification of Ser345 phosphorylation by ERK and p38 MAPK, which represents convergent signalling of the MAPKs leading to neutrophil NADPH oxidase priming at inflammatory sites (Dang *et al*, 2006). The sequence surrounding this phosphorylation site in mouse p47^{phox} is quite different (Figure 7A), and there are three potential phosphorylation sites for p38 MAPK (Xue *et al*, 2006). Through DNA mutagenesis, we individually replaced these sites with alanine, and expressed the resulting mouse p47^{phox} as GST fusion proteins for *in vitro* kinase assay. Ala substitution of Thr356, but not Ser346 and Ser355, resulted in a significant reduction in p38 MAPK-catalysed substrate phosphorylation (Figure 7B). This result suggests that The356 is a site for p38 MAPK phosphorylation.

We then compared C5a-induced p47^{phox} phosphorylation in WT and *Mkp5*$^{-/-}$ neutrophils. After treatment with SB203580 or vehicle control (DMSO) for 15 min, neutrophils were stimulated with C5a for 1 min, and cell lysate was prepared. Phosphorylated proteins were collected using affinity chromatography. The phosphoproteins were separated on SDS–PAGE, transferred to membrane and blotted with an anti-p47^{phox} antibody. As shown in Figure 8, C5a stimulated p47^{phox} phosphorylation in both WT and *Mkp5*$^{-/-}$ neutrophils, with the latter showing a significant increase in p47^{phox} phosphorylation ($P<0.05$). Treatment of neutrophils with SB203580 reduced p47^{phox} phosphorylation by approximately 50%. The partial inhibition of C5a-induced p47^{phox} phosphorylation by SB203580 is expected because other protein kinases, such as PKC, are also activated and can contribute to p47^{phox} phosphorylation (el Benna *et al*, 1994).

Increased superoxide production by Mkp5$^{-/-}$ *neutrophils is essential for the augmented vascular inflammation*

Phagocyte NADPH oxidase is a multi-protein complex consisting of membrane-associated gp91^{phox} (Nox2) and p22^{phox}, cytosolic proteins including p67^{phox}, p47^{phox}, p40^{phox} and the small GTPase Rac (Babior *et al*, 2002). Loss or mutations of the genes coding for these components results in ablated neutrophil superoxide production, which may develop into chronic granulomatous disease (Dinauer and Orkin, 1992; Heyworth *et al*, 2003). Mouse models of chronic granulomatous disease have been established by genetic deletion of the gp91^{phox} gene (Pollock *et al*, 1995) or the p47^{phox} gene (Jackson *et al*, 1995), both lacking the ability for their neutrophils to generate superoxide. To determine whether excessive neutrophil superoxide production underlies the vascular injury in *Mkp5*$^{-/-}$ mice, we generated mice lacking both *Mkp5* and *p47*^{phox}. The double-knockout mice were viable and fertile, but their neutrophils produced little superoxide when stimulated with either C5a (Figure 9A) or PMA (Figure 9B). In the modified LSR model, macroscopic haemorrhage and necrosis at the LPS injection site was markedly reduced in *p47*$^{phox\ -/-}$ *Mkp5*$^{-/-}$ mice (Figure 9C). On microscopic analysis, only moderate oedema was found at the LPS injection site in two of the seven mice (28.5%; Figure 8D, lower right image) and no erythrocyte extravasation and occlusive thrombi were found in the tissue. In contrast, seven of the 8 *p47*$^{phox\ +/+}$ *Mkp5*$^{-/-}$ mice (87.5%) exhibited severe macroscopic haemorrhage within 24 h after receiving a single LPS injection (Figure 9C) and the characteristic histological changes (upper right image in Figure 9D). These results show a correlation between the lack of superoxide production and reduced skin lesions, suggesting an important role of augmented neutrophil oxidant production in the accelerated and robust vascular inflammatory response in

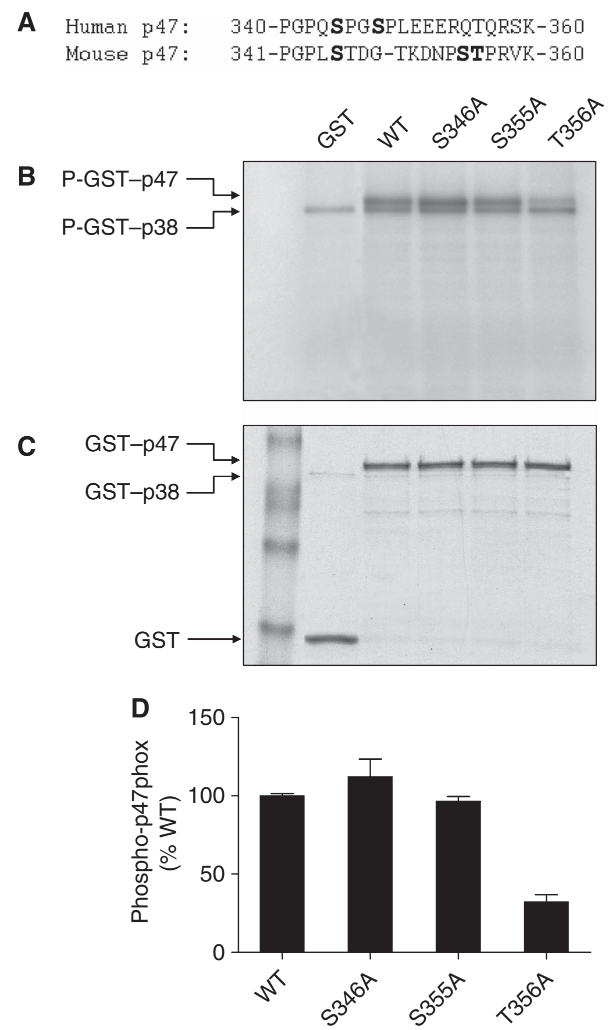

Figure 7 Identification of Thr356 in mouse p47^{phox} as a p38 MAPK phosphorylation site. (**A**) Alignment of sequence of human and mouse p47^{phox} proteins surrounding the potential p38 MAPK phosphorylation site. (**B**) Autoradiograph of *in vitro* kinase assay using full-length WT or mutated mp47^{phox} fused to GST as substrates and an activated GST–p38α, as detailed in the section 'Materials and methods'. GST without mp47^{phox} was used as a negative control. Two phosphorylated bands were identified in the autoradiograph: a phosphorylated GST–mp47^{phox} (apparent molecular weight 72 kDa), and an autophosphorylated GST–p38 (apparent molecular weight 68 kDa). (**C**) Coomassie blue staining showing the positions and levels of the proteins in the gel. (**D**) The extent of substrate phosphorylation was quantified by densitometry, and fold change relative to the phosphorylated WT GST–mp47^{phox} was shown. Two independent kinase assays were performed, and similar results were obtained.

Mkp5$^{-/-}$ mice. Interestingly, the loss of p47^{phox} only produced a small effect on the LPS and TNF-α-induced classic LSR (Supplementary Figure S5), suggesting that different mechanisms contribute to the vascular injury in the classic LSR and the one-injection model.

Discussion

Results from this study illustrate an important physiological function of MKP5 in the protection against LPS-induced tissue injury. Inflammatory stimuli, such as LPS and C5a, have enormous capacity to activate MAPKs, leading to dis-

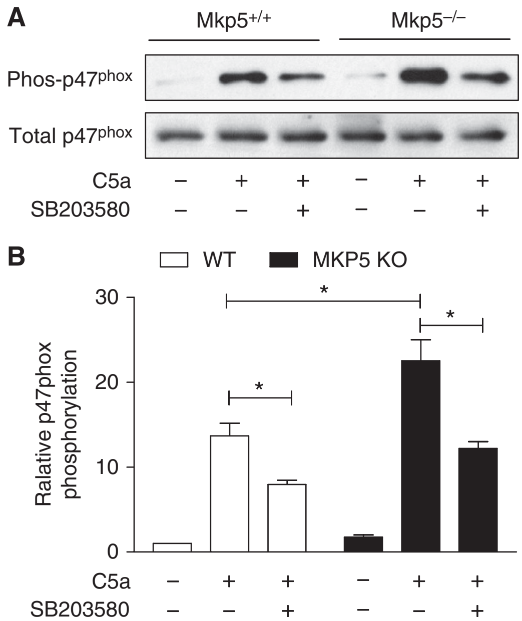

Figure 8 Posphorylation of p47^{phox} in WT and *Mkp5*$^{-/-}$ neutrophils on C5a stimulation. Neutrophils from *Mkp5*$^{-/-}$ and WT littermates were pre-treated with SB203580 (3 μM) or vehicle for 15 min, and then stimulated with C5a (100 nM) for 1 min. The phosphorylated proteins from neutrophil lysate were collected through affinity chromatography as described in the section 'Materials and methods'. (**A**) Western blots showing phosphorylated p47^{phox} (in the eluate) and total p47^{phox} (in the cell lysate), detected with an anti-p47^{phox} antibody. (**B**) Densitometry analysis was conducted to determine the relative level of mouse p47^{phox} phosphorylation based on three independent experiments. *$P<0.05$.

ruption of homeostasis and tissue injury in the absence of an inactivation mechanism. In normal individuals, this inactivation is mediated through the MKPs, which are well suited for this function as they regulate the diverse biological activities of MAP kinases in innate immune cells. Recent studies using genetically altered mice have begun to delineate the *in vivo* functions of selected MKPs. For instance, both *Mkp1*$^{-/-}$ and *Mkp5* $^{-/-}$ mice display enhanced production of inflammatory cytokines (Shepherd *et al*, 2004; Zhang *et al*, 2004; Chi *et al*, 2006), suggesting that these phosphatases regulate transcriptional activation. MKP1 is one of the more extensively investigated MKPs, and its role in regulating host immune response *in vivo* has been reported (Zhao *et al*, 2005, 2006). The activity of MKP1 is affected not only by the activated MAPKs but also through induced expression by stress, growth factors and LPS (Charles *et al*, 1992; Keyse and Emslie, 1992; Zhao *et al*, 2005). In contrast, induced expression is not a mechanism of regulation for several other MKPs including MKP3 and MKP5 (Groom *et al*, 1996; Jeffrey *et al*, 2007), and how these phosphatases are regulated in innate immune cells remains unclear.

In comparison to MKP1, MKP5 has not been extensively studied *in vivo* and little is known about its physiological functions in neutrophils. The initial characterization of the *Mkp5*$^{-/-}$ mice showed an important function of MKP5 in the regulation of T-cell proliferation and activation as well as cytokine production (Zhang *et al*, 2004). Both MKP1 and MKP5 are found in leukocytes including neutrophils and

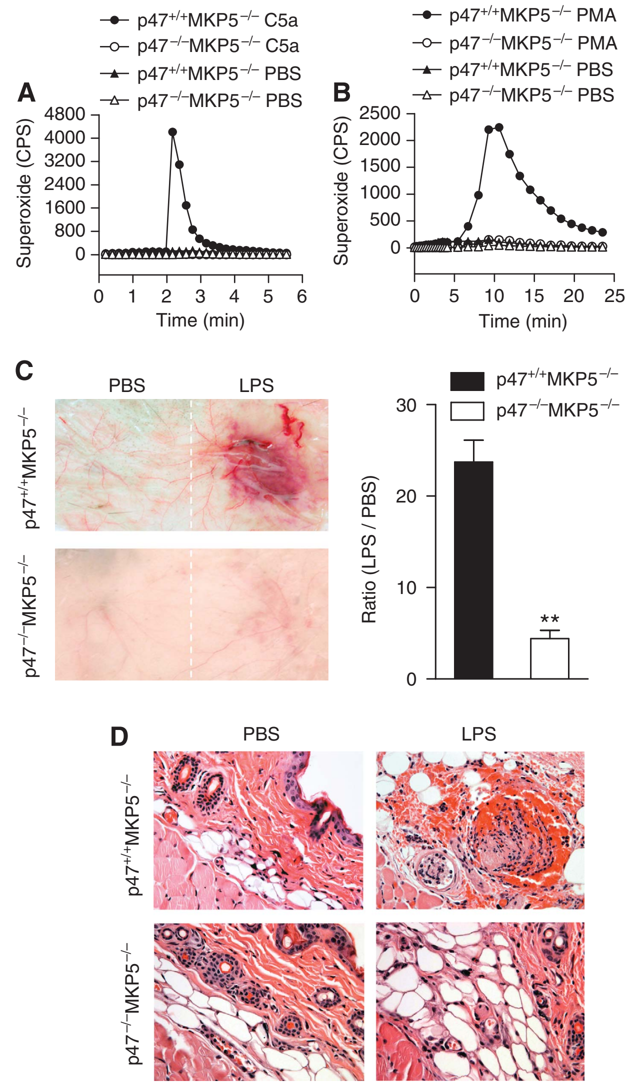

Figure 9 Superoxide production and vascular response in *p47*$^{phox-/-}$ *Mkp5*$^{-/-}$ mice. (**A**) and (**B**) Absence of superoxide production by *p47*$^{phox-/-}$ neutrophils. Bone marrow neutrophils from *p47*$^{phox+/+}$ *Mkp5*$^{-/-}$ and *p47*$^{phox-/-}$ *Mkp5*$^{-/-}$ mice (5×10^5 cells/sample) were stimulated with 100 nM C5a (A) or 200 ng/ml PMA (B), using PBS as a negative control. Superoxide production was shown as counts per second (CPS) in isoluminol-ECL. A representative set of tracings from five similar experiments is shown. (**C**) Representative images showing macroscopic appearance of the LPS injection sites in *p47*$^{phox+/+}$ *Mkp5*$^{-/-}$ mice ($n=8$) and *p47*$^{phox-/-}$ *Mkp5*$^{-/-}$ mice ($n=7$), observed 24 h after s.c. injection with LPS (80 μg) or PBS. The degree of haemorrhage in LPS-injected mice was estimated as described in Figure 1. (**D**) Representative photomicrographs of H&E-stained skin sections from *p47*$^{phox+/+}$ (upper panels) and *p47*$^{phox-/-}$ (lower panels) *Mkp5*$^{-/-}$ mice that received dermal injection with LPS (right side) or PBS (left side). Erythrocyte extravasation and occlusive thrombi containing neutrophils were visible in the sample from *p47*$^{phox+/+}$ *Mkp5*$^{-/-}$ mice but not *p47*$^{phox-/-}$ *Mkp5*$^{-/-}$ mice. Magnification $=\times400$. **$P<0.01$.

macrophages, and they display similar *in vitro* substrate specificities (p38≈JNK>ERK) (Keyse, 2000). Surprisingly, in spite of the similarities between these two MKPs, MKP1 is unable to compensate for the loss of MKP5 in the modified LSR model. These findings suggest that MKP5 has a non-redundant function in regulating LPS-induced vascular inflammatory response. Several differences in the biochemical properties between the two phosphatases may contribute to their functional disparities described here. MKP1 is a member of the Type I DUSP subfamily, which also includes MKP2, MKP3, MKP4 and PAC1 (Farooq and Zhou, 2004; Lang *et al*, 2006; Jeffrey *et al*, 2007; Liu *et al*, 2007). These proteins have similar length (300–400 amino acids) and organization of the substrate-binding and phosphatase domains. In comparison, MKP5 is the only member of the Type III DUSP subfamily that contains an additional NT (N-terminal) domain with unknown functions, although this structure is not critical to the substrate specificity or catalytic activity of MKP5 (Zhang *et al*, 2008). The substrate specificity of MKP1 is similar to that of MKP5, whereas other MKPs such as MKP3 and PAC1 are highly selective for ERK (Ward *et al*, 1994; Groom *et al*, 1996). All MKPs contain a conserved signature sequence in the active site loop of the phosphatase domains, suggesting that they use a similar dephosphorylation mechanism (Denu and Dixon, 1998; Camps *et al*, 2000). On the basis of these published information, we postulate that cellular localization of MKP5 might be critical to its non-redundant function in limiting neutrophil superoxide production. Most MKPs are either nuclear (e.g. MKP1 and PAC1) or cytosolic (e.g. MKP3 and MKP7) proteins. In addition, some MKPs (e.g. MKP4 and MKP5) are found in both nuclear and cytosolic fractions (reviewed in Jeffrey *et al*, 2007; Liu *et al*, 2007). On the basis of our western blotting results, the majority of neutrophil MKP5 is found in the cytosolic fraction (Supplementary Figure S6), although MKP5 is also detected in the nucleus. Therefore, MKP5 is well suited for its regulation of MAPK-catalysed phosphorylation of $p47^{phox}$ (Dang *et al*, 2006), which occurs in neutrophil cytosol and is critical to membrane translocation of the cytosolic components of phagocyte NADPH oxidase (Babior *et al*, 2002; Nauseef, 2004).

Our results show that MKP5 regulation of p38 MAPK is primarily responsible for limiting $p47^{phox}$ phosphorylation, thereby reducing neutrophil superoxide production and ablating the LPS-induced vascular injury in LSR. This notion is supported by the experimental data showing higher level of $p47^{phox}$ phosphorylation in $Mkp5^{-/-}$ neutrophils after C5a stimulation compared with $Mkp5^{+/+}$ neutrophils. Moreover, the p38 MAPK inhibitor, SB203580, decreased the C5a-induced $p47^{phox}$ phosphorylation and superoxide production in isolated mouse neutrophils. When co-administered with LPS into $Mkp5^{-/-}$ mice, SB203580 suppressed ATF-2 phosphorylation and markedly reduced vascular injury in LSR. C5a was used in these experiments because it is known to be generated *in vivo* after LPS administration and has an important function in inflammatory diseases (Guo and Ward, 2005). An earlier study found C5a to be necessary for the development of thrombohaemorrhagic vascular injury in LSR (Rothstein *et al*, 1988). Our results extend this finding and identify activation of p38 MAPK and phosphorylation of $p47^{phox}$ as mechanisms by which C5a contributes to LSR.

In human neutrophils, phosphorylation of $p47^{phox}$ by p38 MAPK results in NADPH oxidase priming at inflammatory sites (Dang *et al*, 2006). To determine whether mouse $p47^{phox}$ is similarly phosphorylated, we conducted *in vitro* kinase assays using WT $p47^{phox}$ and its alanine substituted mutants as substrates. This study resulted in the identification of Thr356 as a phosphorylation site for p38 MAPK. It is still possible that p38 MAPK phosphorylates multiple sites in mouse $p47^{phox}$, based on residual phosphorylation seen with the T356A mutant. It is also interesting to observe a significant contribution of p38 MAPK to the phosphorylation of mouse $p47^{phox}$, as evidenced by a 40–50% reduction in $p47^{phox}$ phosphorylation with SB203580 treatment. This significant reduction may be attributed to several factors, including the presence of more than one p38 MAPK phosphorylation site in mouse $p47^{phox}$, and the involvement of protein kinases downstream of p38 MAPK in $p47^{phox}$ phosphorylation. Additionally, $p47^{phox}$ phosphorylation by p38 MAPK may facilitate its phosphorylation by other kinases, which is consistent with the concept of NADPH oxidase priming that potentiates subsequent activation by another agonist. These possibilities will be examined in future studies, which we expect to lend further support to a critical role for p38 MAPK in NADPH oxidase activation.

Before this study, direct evidence for a role of oxygen radicals in LSR was lacking. A published report indicates that neutrophil elastase, not superoxide, is key to vascular injury in the classical LSR (Hirahashi *et al*, 2006). In contrast, our results have shown that excessive superoxide production by the $Mkp5^{-/-}$ neutrophils is a pre-dominant factor for the augmented LSR after a single injection of LPS. We further show that adoptive transfer of the $Mkp5^{-/-}$ neutrophils to the WT recipients is sufficient to replicate the vascular injury with LPS stimulation, and that LPS failed to induce skin lesions in $p47^{phox-/-}$ $Mkp5^{-/-}$ mice. We observed that $p47^{phox-/-}$ deficiency had a minimal impact on vascular injury in the classic LSR, a finding consistent with the report by Hirahashi *et al* (2006) using $gp91^{-/-}$ mice. Together, these results suggest that different mechanisms are used in the one-injection LSR model and the classic LSR model. Although neutrophil oxidant production is primarily responsible for the vascular injury in the one-injection model, a complement C3-triggered, Mac-1-dependent signalling pathway is the major cause for the thrombohaemorrhagic vascular injury resulting from increased neutrophil elastase release (Hirahashi *et al*, 2006). Therefore, both neutrophil elastase and oxygen radicals are able to cause tissue damage, and either of them may be the pre-dominant factor for vascular injury at the inflammatory sites. In addition to the increased NADPH oxidase activity, MKP5 deficiency can augment neutrophil-mediated vascular injury through enhanced expression of inflammatory factors after LPS stimulation, as evidenced in our air pouch model.

In summary, our experimental data show for the first time that MKP5 provides an essential ‘braking’ mechanism in neutrophil p38 MAPK activation, preferentially suppressing excessive neutrophil superoxide generation and protecting against oxidant-mediated tissue injury. This function of MKP5 is important and cannot be substituted by the functions of other MKPs, such as MKP1, that have similar substrate specificity. Our study provides an *in vivo* example that justifies the presence of multiple MKPs in spite of their overlapping substrate specificities. The results from this study support the concept that intrinsic surveillance is a crucial regulatory mechanism that counteracts the effects of inflammatory stimuli (Nathan, 2002). The current work identifies MKP5 as one such mechanism in neutrophils that prevents excessive production of oxygen radicals when the host is exposed to bacterial products such as LPS, which contributes to septic shock and multi-organ failure in Gramnegative bacterial infection. Identification of mechanisms whereby the MKP5 activity is regulated will benefit the design of therapeutic strategies for maximal elimination of invading microbes while reducing unwanted injury to host tissues.

Materials and methods

Mice

The MKP5-deficient mice were generated and initially characterized as described (Zhang *et al*, 2004). The absence of MKP5 in the knockout neutrophils was confirmed (Supplementary Figure S6). The $p47^{phox}$-deficient mice (Jackson *et al*, 1995) was kindly provided by Dr Steven M Holland (National Institutes of Health, Bethesda, MD). These mice were crossed to generate $p47^{phox+/-}Mkp5^{-/-}$ offspring, which were bred to produce littermates ($p47^{phox-/-}Mkp5^{-/-}$ and $p47^{phox+/+}Mkp5^{-/-}$) for experiments. The MKP1-deficient mice (Dorfman *et al*, 1996) were obtained from Bristol Myers Squibb (Princeton, NJ). WT littermates were used with the knockout mice in paired experiments. All experiments involving mice were conducted using protocols approved by the Institutional Animal Care and Use Committee at the University of Illinois at Chicago.

Modified local Shwartzman reaction

Before LPS injection, age-matched $Mkp5^{+/+}$ and $Mkp5^{-/-}$ littermates of 8–10 weeks were anaesthetized with an i.p. injection of ketamine (100 mg/kg) and xylazine (5 mg/ml) in PBS. The dorsal skin was shaved and 80 μg of *Escherichia coli* LPS (O555:B5, Sigma) in 80 μl PBS was injected in the right dorsum with a Hamilton syringe and a 22G needle. As a negative control, 80 μl sterile PBS was injected in the left dorsum. Twenty-four hours after the LPS injection, mice were euthanized, and the skin was excised for macroscopic examination, histological analysis with haematoxylin and eosin staining and measurement of MPO activity. The relative levels of haemorrhage were quantified by densitometry of macroscopic images, using the ImageJ software (National Institutes of Health).

Myeloperoxidase assay

Frozen mouse skin was homogenized with a Teflon homogenizer in 50 mM phosphate buffer. After centrifugation at 13 000 *g* for 30 min, the cell pellet was resuspended in 1 ml 0.5% hexadecyl trimethylammonium bromide (Sigma), and treated with three cycles of freeze, thaw and sonication. After centrifugation at 13 000 *g* for 20 min at 4°C, the supernatant was incubated with 16 mM 3,3′,5,5′-tetramethylbenzidine (Sigma) and 15 mM H_2O_2, and absorbance at 655 nm was determined. One unit of MPO activity was defined as the change of absorbance of 1.0 per min.

Cytokine secretion

In some experiments, skin air pouch was generated by injection of 4 ml sterile air into the dorsal skin of mice on Day 0. An additional 3 ml air was injected on Day 4 and on Day 7 LPS (80 μg) was injected into the dorsal skin at the air pouch. After 2 h, the air pouch was lavaged with 1 ml ice-cold PBS, and the concentration of cytokines was determined by ELISA (R&D Systems).

Preparation and analysis of mouse neutrophils

Mouse bone marrow cells flushed from femurs and tibias were resuspended in 3 ml Ca^{2+}/Mg^{2+}-free Hank's balanced salt solution (HBSS) containing 1% BSA, which were loaded onto a discontinuous density gradient containing 3 ml of a 72% Percoll under 3 ml of Nyco-prep. After centrifugation at 1000 *g* for 20 min at room temperature, cells at the interface between the 72% Percoll and Nyco-prep were collected and washed with Ca^{2+}/Mg^{2+}-free HBSS. Contaminating erythrocytes were removed with the use of RBC lysis buffer (Sigma), and white blood cells (∼78% neutrophils based on anti-Gr-1 stain) were suspended in Ca^{2+}/Mg^{2+}-free HBSS containing 1% BSA for further assay. In some experiments, peripheral blood was collected by cardiac puncture after CO_2 inhalation. Total and differential leukocyte counts were determined in a Hemavet 950FS multispecies haematology analyser (Drew Scientific).

Superoxide production assays

Superoxide production by mouse neutrophils was determined in an isoluminol-enhanced chemiluminescence (ECL) assay as described earlier (Dahlgren and Karlsson, 1999). Chemiluminescence was measured in a Wallac 1420 Multilabel Counter (PerkinElmer Life Sciences) for 5 min before and 15–30 min after stimulation with agonists or vehicle control. Some samples were pre-treated with the MAPK inhibitors (Calbiochem) for 20 min before agonist stimulation. For superoxide generation by adherent neutrophils, 96 well plates were coated with 100 μg/ml fibrinogen (Sigma) overnight at 4°C before use.

Neutrophil depletion

To deplete neutrophils, mice were intraperitoneally injected with 5 mg/kg (∼100 μg/mouse) anti-Gr-1 antibody (RB6-8C5; eBioscience) 24 h before LPS challenge. Isotype-matched IgG of the same amount was used as a negative control. Peripheral neutrophil count was determined before antibody injection and also 24 and 48 h after the injection.

Adoptive transfer of mouse neutrophils

Neutrophils purified from WT and $Mkp5^{-/-}$ bone marrow were collected and suspended in Ca^{2+}/Mg^{2+}-free HBSS at a concentration of 1×10^7 cells/ml and 5×10^7 cells/ml. Then 200 μl of WT and $Mkp5^{-/-}$ neutrophils were injected through tail vein into a recipient WT mouse 10 min before LPS injection. Twenty-four hours after LPS injection, mice were killed and dorsal skin was excised for photo documentation.

MAPK activation and pharmacological inhibition

Bone marrow neutrophils (1×10^7 cells/sample) were incubated with C5a (10 nM) for varying time intervals. The cells were then collected and lysed in buffer containing 20 mM Tris–HCl, pH 7.6, 150 mM NaCl, 5 mM EDTA, 1 mM Na-orthovanadate, 20 μM 4-(2-aminoethyl)-benzenesulfonyl fluoride, 1% Triton X-100, 5 μg/ml leupeptin, Calbiochem phosphatase inhibitor cocktail and protease inhibitor cocktail. The cell lysate was separated on SDS–PAGE and analysed by western blotting. Phosphorylated and non-phosphorylated forms of the MAPK were detected by specific antibodies against ERK1 and 2 (Thr202/Tyr204), p38 MAPK (Thr180/Tyr182) and JNK (Thr183/Tyr185) (Cell Signaling Technology), and quantified by densitometry analysis using the ImageJ software. To determine the *in vivo* effect of SB203580, 8–10-week-old $Mkp5^{-/-}$ mice were injected s.c. with 80 μg of LPS or LPS mixed with 100 μg of SB203580 HCl (Calbiochem, Cat.559395) in 80 μl of sterile PBS. Twenty-four hours after LPS injection, mice were euthanized and the skin sample was assessed for vascular injury. Skin tissue homogenate was prepared and phosphorylation of ATF-2 was determined with an antibody recognizing the phosphorylated Thr71 in ATF-2 (Cell Signaling Technology).

Phosphorylation of mouse p47phox

Neutrophils from WT and KO mice were pre-treated with 3 μM of SB203580 or buffer control for 15 min, and stimulated with 100 nM of C5a for 1 min. The phosphorylated proteins from cell lysate were collected using affinity chromatography with a phosphoprotein purification kit (Qiagen), as described earlier (Nanamori *et al*, 2007). The eluate containing phosphoproteins and a fraction of the total cell lysate were separated by SDS–PAGE, transferred to membrane and blotted with a polyclonal anti-$p47^{phox}$ antibody (Santa Cruz Biotechnology). Densitometry analysis was conducted to determine the level of $p47^{phox}$ phosphorylation and the level of total $p47^{phox}$ in the cell lysate.

For *in vitro* kinase assay, the coding sequence of full-length mouse WT or mutant $p47^{phox}$ cDNA was fused to a GST gene in the pGEX-4T1 vector (GE Healthcare). The resulting GST–$mp47^{phox}$ fusion construct was expressed in *E. coli* strain BL21 DE3, and purified on glutathione affinity column. *In vitro* kinase assays were performed using activated GST–p38α MAP kinase (Met1-Ser360; Cell Signaling, Cat. 7474). The kinase reaction contained 1 μg of the WT or mutant GST–$mp47^{phox}$ fusion protein, 0.2 μg GST–p38α MAPK and 10 μCi [γ-32P] ATP, and kinase buffer as described (Cheng *et al*, 2007). The autoradiograph was quantified using the ImageGauge software (v.3.12; Fuji Photo Film).

Statistical analysis

Data were expressed as means ± s.e.m. Differences between groups of mice were evaluated with Student's t-test. A P-value <0.05 was considered statistically significant.

Supplementary data

Supplementary data are available at *The EMBO Journal* online (http://www.embojournal.org).

Acknowledgements

We thank Dr Steven Holland for kindly providing the p47^{phox} knockout mice, Dr Jamel El Benna and Dr Qiang Wen for helpful discussions, and Dr Benjamin Ganter for critical reading of the paper. This work was supported in part by grants from National Institutes of Health (R01 AI033503 and P01 HL077806).

Conflict of interest

The authors declare that they have no conflict of interest.

References

Alessi DR, Gomez N, Moorhead G, Lewis T, Keyse SM, Cohen P (1995) Inactivation of p42 MAP kinase by protein phosphatase 2A and a protein tyrosine phosphatase, but not CL100, in various cell lines. *Curr Biol* **5:** 283–295

Babior BM, Lambeth JD, Nauseef W (2002) The neutrophil NADPH oxidase. *Arch Biochem Biophys* **397:** 342–344

Bhalla US, Ram PT, Iyengar R (2002) MAP kinase phosphatase as a locus of flexibility in a mitogen-activated protein kinase signaling network. *Science* **297:** 1018–1023

Brozna JP (1990) Shwartzman reaction. *Semin Thromb Hemost* **16:** 326–332

Camps M, Nichols A, Arkinstall S (2000) Dual specificity phosphatases: a gene family for control of MAP kinase function. *FASEB J* **14:** 6–16

Charles CH, Abler AS, Lau LF (1992) cDNA sequence of a growth factor-inducible immediate early gene and characterization of its encoded protein. *Oncogene* **7:** 187–190

Chen Z, Gibson TB, Robinson F, Silvestro L, Pearson G, Xu B, Wright A, Vanderbilt C, Cobb MH (2001) MAP kinases. *Chem Rev* **101:** 2449–2476

Cheng N, He R, Tian J, Dinauer MC, Ye RD (2007) A critical role of protein kinase C delta activation loop phosphorylation in formyl-methionyl-leucyl-phenylalanine-induced phosphorylation of p47(phox) and rapid activation of nicotinamide adenine dinucleotide phosphate oxidase. *J Immunol* **179:** 7720–7728

Chi H, Barry SP, Roth RJ, Wu JJ, Jones EA, Bennett AM, Flavell RA (2006) Dynamic regulation of pro- and anti-inflammatory cytokines by MAPK phosphatase 1 (MKP-1) in innate immune responses. *Proc Natl Acad Sci USA* **103:** 2274–2279

Dahlgren C, Karlsson A (1999) Respiratory burst in human neutrophils. *J Immunol Methods* **232:** 3–14

Dang PM, Stensballe A, Boussetta T, Raad H, Dewas C, Kroviarski Y, Hayem G, Jensen ON, Gougerot-Pocidalo MA, El-Benna J (2006) A specific p47phox -serine phosphorylated by convergent MAPKs mediates neutrophil NADPH oxidase priming at inflammatory sites. *J Clin Invest* **116:** 2033–2043

Denu JM, Dixon JE (1998) Protein tyrosine phosphatases: mechanisms of catalysis and regulation. *Curr Opin Chem Biol* **2:** 633–641

Dinauer MC, Orkin SH (1992) Chronic granulomatous disease. *Annu Rev Med* **43:** 117–124

Dong C, Davis RJ, Flavell RA (2002) MAP kinases in the immune response. *Annu Rev Immunol* **20:** 55–72

Dorfman K, Carrasco D, Gruda M, Ryan C, Lira SA, Bravo R (1996) Disruption of the erp/mkp-1 gene does not affect mouse development: normal MAP kinase activity in ERP/MKP-1-deficient fibroblasts. *Oncogene* **13:** 925–931

el Benna J, Faust LP, Babior BM (1994) The phosphorylation of the respiratory burst oxidase component p47phox during neutrophil activation. Phosphorylation of sites recognized by protein kinase C and by proline-directed kinases. *J Biol Chem* **269:** 23431–23436

Farooq A, Zhou MM (2004) Structure and regulation of MAPK phosphatases. *Cell Signal* **16:** 769–779

Groom LA, Sneddon AA, Alessi DR, Dowd S, Keyse SM (1996) Differential regulation of the MAP, SAP and RK/p38 kinases by Pyst1, a novel cytosolic dual-specificity phosphatase. *EMBO J* **15:** 3621–3632

Guo RF, Ward PA (2005) Role of C5a in inflammatory responses. *Annu Rev Immunol* **23:** 821–852

Heyworth PG, Cross AR, Curnutte JT (2003) Chronic granulomatous disease. *Curr Opin Immunol* **15:** 578–584

Hirahashi J, Mekala D, Van Ziffle J, Xiao L, Saffaripour S, Wagner DD, Shapiro SD, Lowell C, Mayadas TN (2006) Mac-1 signaling via Src-family and Syk kinases results in elastase-dependent thrombohemorrhagic vasculopathy. *Immunity* **25:** 271–283

Jackson SH, Gallin JI, Holland SM (1995) The p47phox mouse knock-out model of chronic granulomatous disease. *J Exp Med* **182:** 751–758

Jeffrey KL, Brummer T, Rolph MS, Liu SM, Callejas NA, Grumont RJ, Gillieron C, Mackay F, Grey S, Camps M, Rommel C, Gerondakis SD, Mackay CR (2006) Positive regulation of immune cell function and inflammatory responses by phosphatase PAC-1. *Nat Immunol* **7:** 274–283

Jeffrey KL, Camps M, Rommel C, Mackay CR (2007) Targeting dual-specificity phosphatases: manipulating MAP kinase signalling and immune responses. *Nat Rev Drug Discov* **6:** 391–403

Keyse SM (2000) Protein phosphatases and the regulation of mitogen-activated protein kinase signalling. *Curr Opin Cell Biol* **12:** 186–192

Keyse SM, Emslie EA (1992) Oxidative stress and heat shock induce a human gene encoding a protein-tyrosine phosphatase. *Nature* **359:** 644–647

Lang R, Hammer M, Mages J (2006) DUSP meet immunology: dual specificity MAPK phosphatases in control of the inflammatory response. *J Immunol* **177:** 7497–7504

Liu Y, Shepherd EG, Nelin LD (2007) MAPK phosphatases—regulating the immune response. *Nat Rev Immunol* **7:** 202–212

Morrison DK, Davis RJ (2003) Regulation of MAP kinase signaling modules by scaffold proteins in mammals. *Annu Rev Cell Dev Biol* **19:** 91–118

Nanamori M, Chen J, Du X, Ye RD (2007) Regulation of leukocyte degranulation by cGMP-dependent protein kinase and phosphoinositide 3-kinase: potential roles in phosphorylation of target membrane SNARE complex proteins in rat mast cells. *J Immunol* **178:** 416–427

Nathan C (2002) Points of control in inflammation. *Nature* **420:** 846–852

Nauseef WM (2004) Assembly of the phagocyte NADPH oxidase. *Histochem Cell Biol* **122:** 277–291

Nauseef WM (2007) How human neutrophils kill and degrade microbes: an integrated view. *Immunol Rev* **219:** 88–102

Pollock JD, Williams DA, Gifford MA, Li LL, Du X, Fisherman J, Orkin SH, Doerschuk CM, Dinauer MC (1995) Mouse model of X-linked chronic granulomatous disease, an inherited defect in phagocyte superoxide production. *Nat Genet* **9:** 202–209

Rothstein JL, Lint TF, Schreiber H (1988) Tumor necrosis factor/cachectin. Induction of hemorrhagic necrosis in normal tissue requires the fifth component of complement (C5). *J Exp Med* **168:** 2007–2021

Salojin KV, Owusu IB, Millerchip KA, Potter M, Platt KA, Oravecz T (2006) Essential role of MAPK phosphatase-1 in the negative control of innate immune responses. *J Immunol* **176:** 1899–1907

Shepherd EG, Zhao Q, Welty SE, Hansen TN, Smith CV, Liu Y (2004) The function of mitogen-activated protein kinase phosphatase-1 in peptidoglycan-stimulated macrophages. *J Biol Chem* **279:** 54023–54031

Shin HS, Snyderman R, Friedman E, Mellors A, Mayer MM (1968) Chemotactic and anaphylatoxic fragment cleaved from the fifth component of guinea pig complement. *Science* **162:** 361–363

Stetson CA, Good RA (1951) Studies on the mechanism of the Shwartzman-phenomenon; evidence for the participation of polymorphonuclear leucocytes in the phenomenon. *J Exp Med* **93:** 49–63

Sun H, Charles CH, Lau LF, Tonks NK (1993) MKP-1 (3CH134), an immediate early gene product, is a dual specificity phosphatase that dephosphorylates MAP kinase *in vivo*. *Cell* **75:** 487–493

Tanoue T, Moriguchi T, Nishida E (1999) Molecular cloning and characterization of a novel dual specificity phosphatase, MKP-5. *J Biol Chem* **274:** 19949–19956

Theodosiou A, Smith A, Gillieron C, Arkinstall S, Ashworth A (1999) MKP5, a new member of the MAP kinase phosphatase family, which selectively dephosphorylates stress-activated kinases. *Oncogene* **18:** 6981–6988

Ward Y, Gupta S, Jensen P, Wartmann M, Davis RJ, Kelly K (1994) Control of MAP kinase activation by the mitogen-induced threonine/tyrosine phosphatase PAC1. *Nature* **367:** 651–654

Xue Y, Li A, Wang L, Feng H, Yao X (2006) PPSP: prediction of PK-specific phosphorylation site with Bayesian decision theory. *BMC Bioinformatics* **7:** 163

Zhang Y, Blattman JN, Kennedy NJ, Duong J, Nguyen T, Wang Y, Davis RJ, Greenberg PD, Flavell RA, Dong C (2004) Regulation of innate and adaptive immune responses by MAP kinase phosphatase 5. *Nature* **430:** 793–797

Zhang Y, Dong C (2007) Regulatory mechanisms of mitogen-activated kinase signaling. *Cell Mol Life Sci* **64:** 2771–2789

Zhang YY, Mei ZQ, Wu JW, Wang ZX (2008) Enzymatic activity and substrate specificity of mitogen-activated protein kinase p38alpha in different phosphorylation states. *J Biol Chem* **283:** 26591–26601

Zhao Q, Shepherd EG, Manson ME, Nelin LD, Sorokin A, Liu Y (2005) The role of mitogen-activated protein kinase phosphatase-1 in the response of alveolar macrophages to lipopolysaccharide: attenuation of proinflammatory cytokine biosynthesis via feedback control of p38. *J Biol Chem* **280:** 8101–8108

Zhao Q, Wang X, Nelin LD, Yao Y, Matta R, Manson ME, Baliga RS, Meng X, Smith CV, Bauer JA, Chang CH, Liu Y (2006) MAP kinase phosphatase 1 controls innate immune responses and suppresses endotoxic shock. *J Exp Med* **203:** 131–140